JOURNAL OF CATALYSIS 113, 307–316 (1988)

CO_2 and NO Chemisorptions on Mo/γ-Al_2O_3 Catalysts

CHI-LIN O'YOUNG,[1] CHAU-HWA YANG, STEPHEN J. DECANIO, MAHENDRA S. PATEL, AND DAVID A. STORM

Texaco Incorporated, P.O. Box 509, Beacon, New York 12508

Received November 9, 1987; revised February 23, 1988

CO_2 and NO chemisorptions, FT-IR, and TGA techniques were used to study the surface structure of calcined and reduced Mo/γ-Al_2O_3 catalysts. The results clearly show that there are three distinct surface structures whose presence is dependent on the molybdenum loading. At low loadings, molybdenum interacts strongly with the alumina surface hydroxyl groups to form "strong Mo interaction species." The molybdenum is highly dispersed, difficult to reduce, and has a low coordination number (C.N.). At medium loadings before the monolayer coverage, the Mo–O–Mo interaction increases and the Mo–support interaction may decrease to form "Mo interaction species." Such formed molybdenum is well dispersed, reducible, and has a high C.N. The CO_2 uptake at the monolayer coverage is almost zero. Above the monolayer coverage, excess molybdenum aggregates to form bulk MoO_3 and $Al_2(MoO_4)_3$ species at the expense of a small amount of well-dispersed molybdenum species to create some exposed alumina surface. The molybdenum formed under this condition is easily reduced, has a large particle size, and has a high C.N. The bulk MoO_3 species interacts with the support to form $Al_2(MoO_4)_3$ at high calcination temperatures (≥600°C). All the molybdenum phases rearrange and agglomerate to create some free alumina and to decrease the molybdenum dispersion after H_2 reduction. The extent of rearrangement and agglomeration depends on the degree of reduction. At low loadings, only a small fraction of free alumina is recovered because of the low reducibility. A significant amount of free alumina is recovered at medium and high loadings due to the high reducibility.

INTRODUCTION

Molybdena–alumina catalysts are used in many important reactions such as hydrotreating, hydrodesulfurization, hydrogenation, and polymerization (*1*). Recently, it has been reported that these catalysts can also be used in syngas catalysis (*2*) and emission control catalysis (*3*). Because of their importance and versatility, the catalysts have been studied extensively. Different characterization techniques have been applied to investigate the surface structure of molybdena catalysts. NO and CO_2 chemisorptions are important and useful techniques which have been employed by Segawa and Hall (*4–6*). They found that NO adsorbed selectively on the molybdena portion of reduced Mo/γ-Al_2O_3 catalysts, while CO_2 adsorbed only on the free alumina portion. Most of their studies were concentrated on one standard sample, 8% Mo catalyst with a monolayer coverage for their support. The extent of reduction was controlled by varying the temperature and time of reduction. Catalysts with different molybdenum loadings have also been studied by different groups (*7–10*). To extend and supplement the studies, a series of Mo/γ-Al_2O_3 catalysts with a wide range of molybdenum loadings was investigated by using NO and CO_2 chemisorptions, FT-IR, and TGA techniques. Rather than focusing on a standard sample and varying the reduction conditions, we studied catalysts with a variety of molybdenum loadings and employed a standard reduction condition (500°C reduction for 3 h). The effect of the molybdenum loading on the physical properties of catalysts was stressed. The results

---

[1] To whom correspondence should be addressed.

0021-9517/88 $3.00

were discussed and compared with those reported in the literature.

EXPERIMENTAL SECTION

Catalysts

A series of Mo/γ-Al_2O_3 catalysts with different molybdenum loadings was prepared by an aqueous incipient wetness impregnation method. Ammonium heptamolybdate, $(NH_4)_6Mo_7O_{24} \cdot 4H_2O$, was used as the molybdenum salt. Norton 6375 γ-Al_2O_3 with a surface area of 216 m^2/g and a pore volume of 1.1 cc/g was used as the support. Aqueous solutions of $(NH_4)_6Mo_7O_{24}$ with desired concentrations were prepared without a pH adjustment. All catalysts were prepared by a single impregnation, dried at 120°C for 16 h, and calcined at 500°C, or 600°C, for 3 h under a stream of air (60 cc/min).

TGA Reduction Studies

The reducibility of Mo/γ-Al_2O_3 catalysts was studied by TGA techniques (*11*). A DuPont 1090 thermal analyzer system was used to measure the weight loss of catalysts during H_2 reduction. The instrument has a weight sensitivity of 5×10^{-3} mg. Samples (about 35 mg) were loaded in a platinum pan. A stream of dried helium, 50 cc/min, was passed through the system; the samples were then heated to 120°C for 1 h to remove physically adsorbed moisture. The samples were further heated to the reduction temperature (400 or 500°C) and held at that temperature until a constant weight was observed. A stream of hydrogen, 50 cc/min, mixed with the helium stream was then introduced to reduce the samples. The weight loss during the reduction was recorded. The reducibility, α, was defined based on the reaction

$$Mo^{6+}O_3 + H_2 \rightarrow Mo^{4+}O_2 + H_2O \quad (1)$$

An α value of 100% means all the $Mo^{6+}O_3$ is reduced to $Mo^{4+}O_2$ and dehydrated. α is equivalent to $\square$/Mo, anion vacancies per Mo atom, as defined in the literature (*12, 13*).

Volumetric Chemisorption Measurements

A conventional volumetric adsorption apparatus (*14*) was used to measure NO and CO_2 chemisorptions at room temperature. AGL NO (nominal purity 99%) and CO_2 were further purified by a molecular sieve trap and a standard freeze–pump–thaw technique. Catalysts were calcined or reduced at 400 or 500°C for 3 h, evacuated to 10^{-5} Torr (1 Torr = 133.3 N/m^2) at 500°C for 1 h, and cooled to room temperature for mesurements. Total and reversible adsorption isotherms at six equilibrium pressures up to 500 Torr were recorded. The actual uptakes were calculated by extrapolating the adsorption isotherms to zero pressure.

FT-IR Studies

IR spectra were collected using a Nicolet 7199 FT-IR spectrophotometer with an MCT detector operating at 77°K. A standard quartz IR cell with a vacuum line was employed. The cell could be heated to 500°C under a vacuum of 10^{-6} Torr. About 20 mg of the catalyst was pressed at 600 psi to form a 1.6-cm-diameter wafer. The procedures used to pretreat wafers and to purify NO and CO_2 were the same as those described previously. NO and CO_2 adsorption were carried out at the ambient temperature. IR spectra were recorded, after physisorbed NO or CO_2 had been evacuated, and were corrected by subtracting the catalyst background. All spectrum subtractions and peak integrations were done by a Nicolet 1180 computer.

RESULTS AND DISCUSSION

BET, XRD, and Reducibility Studies

Results of BET(N_2) surface area, XRD, and reducibility studies are shown in Table 1. The surface area of 500°C calcined samples decreases with the molybdenum loading. This decrease is not due to the effect of sintering, because the calculated surface areas based on the alumina content alone are very close to the measured sur-

TABLE 1

Surface Area, XRD, and Reducibility of Catalysts

% Mo	S. A. (m^2/g)		XRD[b]	Reducibility[c]	
	Exp.	Cal.[a]		at 400°C (%)	at 500°C (%)
0.0[d]	216.0[e]	216.0	No bulk phase	0.00	0.00
1.0	214.0	212.8	No bulk phase	0.00	0.00
2.0	212.0	209.5	No bulk phase	0.00	0.00
3.0	211.9	206.3	No bulk phase	0.00	0.00
6.0	206.3	196.6	No bulk phase	0.00	40.90
9.0	195.2	186.8	No bulk phase	17.85	56.95
12.0	183.2 163.5[f]	177.1	MoO_3 (m), $Al_2(MoO_4)_3$ $Al_2(MoO_4)_3$(m), MoO_3	32.71	86.04
15.0	170.3 152.0[f]	167.4	MoO_3 (m), $Al_2(MoO_4)_3$ $Al_2(MoO_4)_3$(m), MoO_3	51.53	100.22
MoO_3				0.00	101.25
$Al_2(MoO_4)_3$				0.00	155.72

[a] Calculated surface areas if only the support is counted.

[b] γ-Al_2O_3 phase was detected in all samples; m, major phase.

[c] Measured by TGA after 3 h of reduction.

[d] Blank γ-Al_2O_3.

[e] Samples calcined at 500°C for 3 h, unless otherwise noted.

[f] Calcined at 600°C for 3 h.

face areas (see Table 1). The effect of sintering can be observed at a high calcination temperature (600°C) as shown in the cases of 12 and 15% Mo samples. It is believed that the alumina support would lose some surface area by sintering only at higher temperatures (>500°C).

The XRD results indicate that γ-Al_2O_3 is the only bulk phase present at low molybdenum loadings (≤9% Mo). At higher loadings (≥12% Mo), bulk MoO_3 and $Al_2(MoO_4)_3$ phases are detected. Bulk MoO_3 is the dominant X-ray observable phase on the samples of 12 and 15% after being calcined at 500°C. It interacts with the support to form $Al_2(MoO_4)_3$ at high calcination temperatures, ≥600°C (*15*). The absence of detectable bulk phases on the low loading samples (1 to 9%) suggests that the molybdenum could be well dispersed on the support (*16*).

In the TGA experiments, the reduction process was nearly completed (about 80% of the weight loss) in the first few hours after hydrogen was introduced. The weight loss continued very slowly, however, even after 24 h or reduction. This phenomenon has been reported in the literature (*11*, *17*). For the sake of convenience, we used 3 h as a standard reduction time. As shown in Table 1, only high loading samples (>9% Mo) have a measurable weight loss during the reduction process at 400°C. At 500°C, three different ranges of reducibility are observed depending on the molybdenum loading: at low loadings (≤3% Mo), no weight loss is detected during the reduction; at medium loadings (6 and 9% Mo) below the monolayer coverage, about 50% reducibility is observed; and at high loadings (>12% Mo), about 100% reducibility is observed. The model compounds, MoO_3 and $Al_2(MoO_4)_3$, are not reducible at 400°C, but have a reducibility of 101.25 and 155.72% at 500°C, respectively. $Al_2(MoO_4)_3$ has a reduction curve similar to that of the catalysts; i.e., most of the reduction was completed in the first few hours, while MoO_3 has a reduction curve in which the weight loss decreased linearly with time

TABLE 2

Results of Reduction Studies of Mo/γ-Al_2O_3 Catalysts

Surface area of support (m^2/g)	% Mo	Reduction conditions		α (%)	e/Mo	Ref.
		Temp. (°C)	Time (min)			
192	8.0(9.0)[a]	500	120	59.3	1.62	Hall (1974)
		400	20	16.6	0.66	
192	8.0(9.0)	500	120	51.2	1.56	Hall (1977)
		400	75	26.5	1.03	
183	7.8(9.2)	500	120	75.0		Chung (1980)
	4.7(5.5)	500	120	48.0		
	3.0(3.5)	500	120	24.0		
	2.0(2.4)	500	120	9.0		
230	8.3(7.8)	490	60	45.3		Ratnasamy (1975)
		510	60	55.3		
		530	60	68.9		
216	9.0	500	180	56.95		This work
		400	180	17.85		
	6.0	500	180	40.90		

[a] Equivalent molybdenum loadings on our support.

and leveled off after 7 h of reduction. It is postulated that the high reducibility of the 12 and 15% Mo samples at 500°C is due to the presence of the bulk MoO_3 and $Al_2(MoO_4)_3$ phases.

The reducibility and XRD data suggest that at low loadings, molybdenum interacts strongly with the support to form a highly dispersed phase. It is probably an isolated monomeric species with a tetrahedral symmetry as suggested (*17*, *18*), and it is difficult to reduce. At medium loadings before the monolayer coverage, the molybdenum is well dispersed. The formation of Mo–O–Mo bonds, which has been shown by Raman spectra (*18*), converts the structure to a polymeric structure with an octahedral symmetry. The Mo–support interaction may also be decreased. The increase in reducibility may be due to the weaker Mo–support interaction or the nature of the polymeric structure. Above the monolayer coverage, excess molybdenum forms easily reducible bulk MoO_3 and $Al_2(MoO_4)_3$ phases. Similar results have been reported in the literature (*11–13*, *17*), and they are compared to our data in Table 2. Chung and Massoth's (*17*) and Ratnasamy's *et al.* (11) data were obtained by TGA techniques, while Hall's *et al.* (*12*, *13*) data were obtained by measuring the water collection in a cold trap. The extent of reduction, e/Mo, as defined in the literature (*12*) cannot be obtained by TGA techniques, but a correlation between α (or □/Mo) and e/Mo has been developed by Hall and Lo Jacono (*13*). Our data supplement those presented and are quite consistent with them if the support surface area is taken into account. For example, the 8% Mo standard sample used by Hall's group had an α = 51.2 or 59.3% at 500°C for 2 h, and an α = 16.6% at 400°C for 20 min (*12*, *13*). Our 9% Mo sample, which is equivalent to the standard sample, has an α = 56.95% at 500°C for 3 h and an α = 17.85% at 400°C for 3 h. For the low loading samples ($\leq$3% Mo), no weight loss is observed probably due to the limit of our instrument sensitivity. For the high loading samples (12 and 15% Mo), high reducibilities are observed due to the formation of bulk phases.

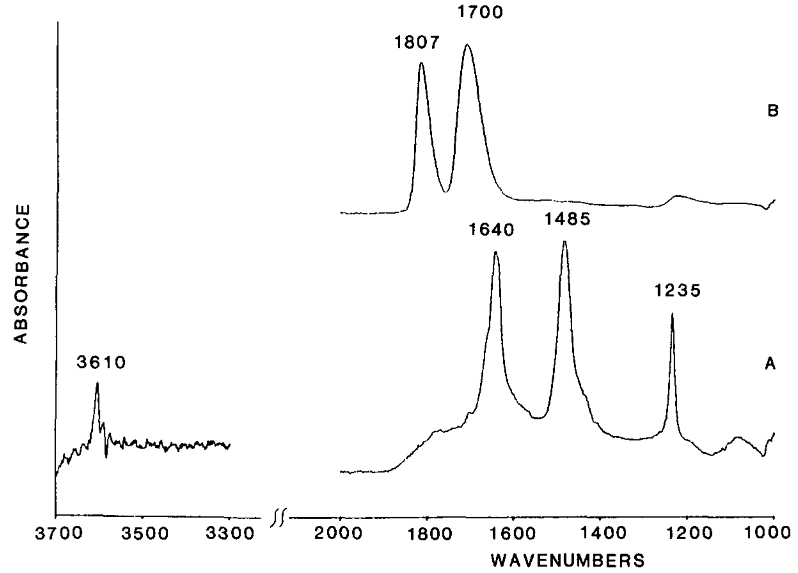

FIG. 1. (A) IR spectrum of CO_2 adsorbed on 500°C calcined γ-Al_2O_3. (B) IR spectrum of NO adsorbed on 500°C reduced 9% Mo/γ-Al_2O_3.

CO_2 Chemisorption and IR Studies

Results of CO_2 chemisorption on 500°C calcined and reduced catalysts at room temperature are shown in Table 3. Since CO_2 adsorbs only on the alumina support (*4*), the irreversible CO_2 uptake per square meter of surface area can be used to calculate the fraction of the uncovered alumina. The reduced alumina support has about 20% higher irreversible CO_2 uptake than the calcined support as shown in the table. Therefore, the fraction of the free alumina of reduced catalysts is better calculated based on the uptake of the reduced support rather than the calcined support. IR spectra of CO_2 adsorbed on the alumina support and catalysts reveal four distinct peaks at 3610, 1644, 1485, and 1235 cm^{-1} (see Fig. 1A). These peaks were assigned to the OH stretch, asymmetric CO stretch, symmetric CO stretch, and C–O–H bending modes of bicarbonate species, respectively (*4*, *19*). The reduced support has higher peak intensities than the calcined support as we observed in the chemisorption study. Using the integrated peak intensity at 1485 cm^{-1}, the fraction of free alumina as a function of molybdenum loading can be calculated. Figure 2 shows both chemisorption and IR data. Both data are quite agreeable for the calcined samples, but not for the reduced samples. This discrepancy could be due to the change of refractive index of catalysts after H_2 reduction. Nevertheless, the overall trends are in a good agreement.

For the calcined catalysts, the fraction of free alumina decreases very fast at low

TABLE 3

CO_2 Chemisorption on Calcined and Reduced Catalysts

% Mo	Calcined catalysts		Reduced catalysts[a]	
	Irreversible uptake (cc-STP/m^2)	% of Free alumina	Irreversible uptake (cc-STP/m^2)	% of Free alumina
0.0	1.216×10^{-2}	100.00	1.458×10^{-2}	100.00
1.0	9.319×10^{-3}	76.64	1.210×10^{-2}	82.99
2.0	5.909×10^{-3}	48.59	9.859×10^{-3}	67.62
3.0	3.731×10^{-3}	30.68	5.898×10^{-3}	40.44
6.0	8.829×10^{-4}	7.26	3.897×10^{-3}	26.72
9.0	0	0	3.191×10^{-3}	21.88
12.0	9.585×10^{-5}	0.79	4.864×10^{-3}	33.35
15.0	4.566×10^{-4}	3.75	5.007×10^{-3}	34.34

[a] All samples were reduced at 500°C for 3 h.

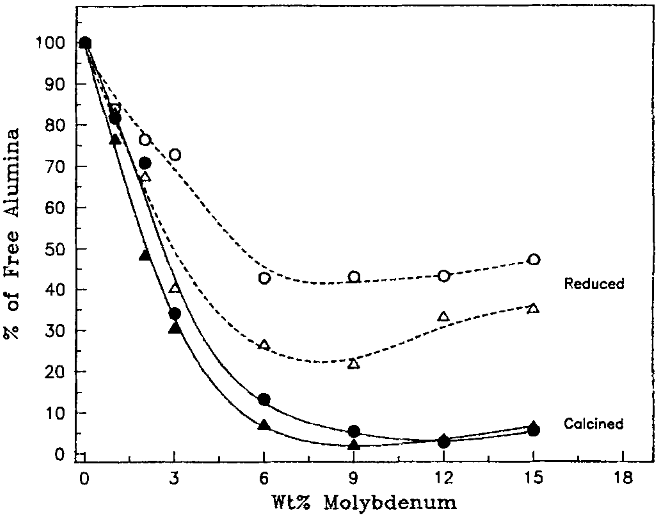

FIG. 2. Fraction of free alumina of 500°C calcined and reduced catalysts based on CO_2 adsorption. (○) IR results of reduced catalysts, (△) chemisorption results of reduced catalysts, (●) IR results of calcined catalysts, (▲) chemisorption results of calcined catalysts.

loadings (≤3%), then goes slowly to zero at 9% Mo, and finally increases slightly after the monolayer coverage. These results suggest that molybdenum interacts more effectively with the surface hydroxyl groups to cover the support at low loadings (≤3%). At medium loadings before the monolayer coverage, the number of alumina hydroxyl groups interacted with molybdenum decreases. As discussed previously, this could be due to the formation of polymeric Mo–O–Mo bonds or the decrease in Mo–support interaction. As a result, the fraction of free alumina decreases slowly and eventually to zero at the monolayer coverage. Above the monolayer coverage, some well-dispersed Mo species migrate to the top of the surface and create a small fraction of free alumina.

For the reduced catalysts, the fraction of free alumina varies with the molybdenum loading in the same way as the calcined catalysts. The reduced catalysts, however, have a higher fraction of free alumina over the calcined catalysts. This indicates that the molybdenum phases rearrange and agglomerate after H_2 reduction. The extent of agglomeration depends on the degree of reduction: at low loadings, only a small fraction of free alumina is recovered because of the low reducibility; at medium and high loadings, a significant amount of free alumina is recovered due to the high reducibility.

CO_2 chemisorption on the standard 8% Mo catalyst has been studied thoroughly by Hall *et al.* (*4–6*). It was found that the fraction of free alumina increased linearly with the extent of reduction after e/Mo = 0.5. A maximum of 50% free alumina recovery was found when the catalyst was fully reduced. Using the correlation between α and e/Mo developed in the literature (*13*), the extent of reduction (e/Mo) of our 9% Mo sample is about 1.56. From this e/Mo value, the fraction of free alumina recovery would be about 37% according to the data of Hall co-workers (*6*). However, our 9% Mo sample has 22% free alumina recovery after being reduced at 500°C for 3 h. This discrepancy is probably due to the different basis we used in the calculations. As discussed previously, the surface hydroxyl groups were regenerated after H_2

reduction; therefore it is more appropriate to use the reduced support as a basis rather than the calcined support.

In conclusion, our results are similar to those of Hall *et al.* (*4–6*). Furthermore, we observe that above the monolayer coverage (>9% Mo) (i) the support is not fully covered by the excess molybdenum, and (ii) the fraction of the free alumina recovery is significant after H_2 reduction.

NO Chemisorption and IR Studies

Table 4 shows the results of NO chemisorption and IR spectral parameters of the reduced catalysts. IR spectra (Fig. 1B) of NO adsorbed on the reduced catalysts show two strong peaks at 1807 and 1700 cm^{-1}. These peaks were assigned as the symmetric and asymmetric stretches of $Mo(NO)_2$, respectively (*20, 21*). Both peak intensities increase with the molybdenum loading, and peak positions are independent of the loading. The NO/Mo ratio and the NO uptake as a function of the loading are shown in Fig. 3. Both chemisorption and IR data show that the NO uptake is low at low loadings, increases fast with the loading up to 9%, and then levels off at high loadings. The NO/Mo ratio is low at low loadings, reaches a maximum of 0.376 at medium loadings, and then decreases at high loadings. These results are consistent with those of the reducibility and XRD experiments of this study. The NO uptake is low at low loadings because of the low reducibility. The NO/Mo ratio, however, is not low because the molybdenum dispersion is high. This moderate NO/Mo ratio implies that even the highly dispersed Mo, found on low loading materials, is reducible. However, the minute reducibility does

TABLE 4

NO Chemisorption and IR Spectral Parameters of Reduced Catalysts

% Mo	Irreversible uptake (cc-STP/g-cat.)	NO/Mo	NO/□	Bond angle, θ	
				500°C red.	400°C red.
1.0	0.542	0.231	ND[a]	110.9	—
2.0	0.868	0.186	ND	109.5	—
3.0	1.668	0.238	ND	109.0	116.0
6.0	5.195	0.371	0.91	105.7	112.7
9.0	7.872	0.376	0.66	105.0	110.5
12.0	9.181	0.328	0.38	105.4	109.3
15.0	10.623	0.303	0.30	—	108.4

[a] ND, not determinable.

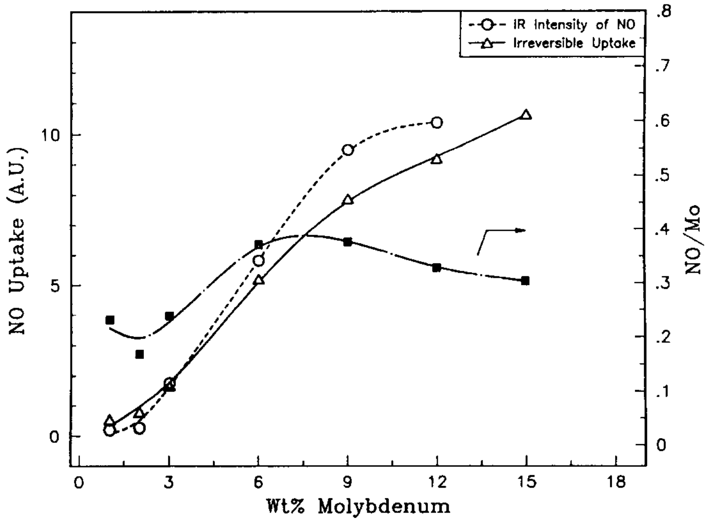

FIG. 3. NO uptake and NO/Mo ratio of 500°C reduced Mo/γ-Al_2O_3 catalysts as a function of molybdenum loading. (○) IR data, (△) chemisorption data.

not warrant an observable weight loss by the TGA technique. At medium loadings, the uptake and the NO/Mo ratio increase because the molybdenum is well dispersed and reducible. Above the monolayer coverage, the uptake levels off and the NO/Mo ratio decreases due to the formation of bulk phases. The dispersion of reduced catalysts is better reflected by the ratio NO/□. The maximum value would be 2 if NO is doubly adsorbed. The extent of reduction has no effect on the NO/□ value. As shown in Table 4, the NO/□ ratio decreases with the loading, indicating that the dispersion of reduced catalysts decreases with the loading.

NO chemisorption on Mo/γ-Al_2O_3 catalysts has been previously studied (*7*, *10*, *22–23*). Jung *et al.* (*7*) observed a very small amount of NO chemisorbed on calcined catalysts. This low uptake was attributed to the NO chemisorption on the exposed alumina surface. Hall *et al.* (*22*) also reported similar results. They found that this small amount of NO uptake could be a significant fraction of the total uptake at low loadings. Taking this into consideration, the actual NO/Mo ratios of our low loading samples might even be lower than those shown in Table 4. Yao (*10*) studied catalysts with various molybdenum loadings and employed a standard reduction condition (500°C, 1 h). He observed a saturation concentration of MoO_3 in the dispersed phase: before the saturation concentration, the NO uptake increased logarithmically with the molybdenum loading, while above the saturation concentration the uptake leveled off. Our results are consistent with his observations. Caceres *et al.* (*23*) studied catalysts with different molybdenum loadings and with the same reducibility (α = 0.92 to 0.95). They observed that NO/Mo decreased with the molybdenum loading. This is consistent with the observation presented here; i.e., NO/□ decreases with the molybdenum loading. NO/□ instead of NO/Mo values are used for the comparison because our samples have different α's. Valyon and Hall (*24*) used different procedures to measure the NO chemisorption at a constant pressure and obtained the NO uptake by extrapolating to zero time. Their standard 8% Mo sample had α = 50%, NO/Mo = 0.37, NO/□ = 0.71, and θ = 103° after reduced at 500°C for 1 h, which was quite comparable to α = 56.95%, NO/Mo = 0.376, NO/□ = 0.66, and θ = 105° obtained for our 9% Mo sample reduced at 500°C for 3 h.

Using the peak intensity ratio of the symmetric and asymmetric NO IR bands, $r = I_{sym}/I_{asym}$, the bond angle θ between the two N–O oscillators can be calculated by the equation $r = \cot^2(\theta/2)$ (*25*). As shown in Table 4, the bond angle of 500°C reduced catalysts is about 110° at low loadings. It decreases slightly to 105° at medium and high loadings. The bong angle of 400°C reduced catalysts has about the same trend, except that it is higher by about 4 to 7°. Again, these results can be interpreted by the surface structures of molybdenum phases. At low loadings, the molybdenum is highly dispersed and has a low coordination number and a tetrahedral symmetry. Therefore, the bond angle of the NO dimer is large because of less crowding. At medium and high loadings, the Mo–support interaction decreases and the Mo–O–Mo interaction increases to form polymeric molybdenum species with an octahedral symmetry. The bond angle decreases because of the high coordination number of Mo. The bond angle of 500°C reduced catalysts is smaller than that of 400°C reduced catalysts because the extent of agglomerization is higher for the 500°C reduced catalysts. Caceres *et al.* (*23*) have observed that the bond angle θ decreased slightly with the molybdenum loading as we have observed. The θ's (between 102° and 97°) were lower than those obtained here because the reducibility of their catalysts was higher (α = 0.92 to 0.95). Higher reducibility of molybdenum leads to agglomerization and low θ's. The effect of NO coverage on the bond angle has been studied by different groups (*26*, *27*). It was found that the bond angle was high at low coverages and decreased with the increasing coverage. The results were interpreted as due to the site crowding and molybdenum agglomerization after H_2 reduction. In summary, all these studies suggest that the bond angle is determined by the molybdenum dispersion, reducibility, and NO coverage.

CONCLUSIONS

These results clearly show that for Mo/γ-Al_2O_3 catalysts, there are three distinct surface structures whose presence is dependent on the molybdenum loading. At low loadings, molybdenum interacts intensely with the alumina hydroxyl groups to form "strong Mo interaction species." This molybdenum is highly dispersed, is difficult to reduce, and has a low C.N., probably a tetrahedral symmetry. At medium loadings up to the monolayer coverage, the Mo–O–Mo interaction increases and the Mo–support interaction may decrease to form "Mo interaction species." The molybdenum is well dispersed, reducible, and has a high C.N., probably an octahedral symmetry. At high loadings after the monolayer coverage, excess molybdenum aggregates to form bulk MoO_3 and $Al_2(MoO_4)_3$ species at the expense of a small amount of well-dispersed molybdenum species. The molybdenum is easily reduced, has a large particle size, and has a high C.N. All the molybdenum phases rearrange and agglomerate to create some free alumina after H_2 reduction. The extent of rearrangement and agglomeration depends on the degree of reduction. At low loadings, only a small fraction of free alumina is recovered because of the low reducibility. At high loadings, a significant amount of free alumina is recovered due to the high reducibility.

ACKNOWLEDGMENTS

We thank Texaco Inc. for permitting us to publish this article; R. Pugliese, R. J. Barresi, J. E. Broas, W. A. McDonald, and M. A. Behrens for their experimental assistance; Dr. K. J. Chou for his discussions; and Professor W. K. Hall for his comments.

REFERENCES

1. For review articles see (*a*) Massoth, F. E., *in* "Advances in Catalysis" (D. D. Eley, H. Pines, and P. B. Weisz, Eds.), Vol. 27, p. 265. Academic Press, New York, 1978; (*b*) Ratnasamy, P., and Sivasanker, S., *Catal. Rev. Sci. Eng.* **22,** 401(1980); (*c*) Haber, J., "The role of Molybdenum in Catalysis." Climax Molybdenum Co., London, 1981.

2. Tatsumi, T., Muramatsu, A., and Tominaga, H., *J. Catal.* **101,** 553 (1986).

3. Gandhi, H. S., Yao, H. C., and Stepien, H. K., ACS "Symposium Series No. 178, Catalysis under Transient Conditions" (A. T. Bell and L. L. Hegedus, Eds.), p. 143. 1981.

4. Segawa, K.-I., and Hall, W. K., *J. Catal.* **77,** 221 (1982).

5. Hall, W. K., *in* "Proceedings, 4th International Conference on the Chemistry and Uses of Molybdenum," p. 224. Climax Molybdenum Co., Ann Arbor, MI, 1982.

6. Milliam, W. S., Segawa, K.-I., Smrz, D., and Hall, W. K., *Polyhedron* **5,** 169 (1986).

7. Jung, H. J., Schmitt, J. L., and Ando, H., *in* "Proceedings, 4th International Conference on the Chemistry and Uses of Molybdenum," p. 246. Climax Molybdenum Co., Ann Arbor, MI, 1982.

8. Massoth, F. E., and Murali Dhar, G., *in* "Proceedings, 4th International Conference on the Chemistry and Uses of Molybdenum," p. 343. Climax Molybdenum Co., Ann Arbor, MI, 1982.

9. Burch, R. and Collins, A., *in* "Proceedings, 4th International Conference on the Chemistry and Uses of Molybdenum," p. 379. Climax Molybdenum Co., Ann Arbor, MI, 1982.

10. Yao, H. C., *J. Catal.* **70,** 440 (1981).

11. Ratnasamy, P., Ramaswamy, A. V., Banerjee, K., Sharma, D. K., and Ray, N., *J. Catal.* **38,** 19 (1975).

12. Hall, W. K., and Massoth, F. E., *J. Catal.* **34,** 41 (1974).

13. Hall, W. K., and Lo Jacono, M., *in* "Proceedings, 6th International Congress on Catalysis, London, 1976" (G. C. Bonds, P. B. Wells, and F. C. Tomkins, Eds.), Vol. 1, p. 246. The Chemical Society, London, 1977.

14. ASTM designation D 3908-80.

15. A minimum temperature of salt formation between MoO_3 and γ-Al_2O_3 has been reported to be 535°C. See Sonnemans, J., and Mars, P., *J. Catal.* **31,** 209 (1973).

16. It is also possible that the crystallite size is below the XRD detection limit.

17. Chung, K. S., and Massoth, F. E., *J. Catal.* **64,** 320 (1980).

18. Jeziorowski, Helge, and Knozinger, Helmut, *J. Phys. Chem.* **83,** 1166 (1979).

19. Darkyns, N. D., *J. Chem. Soc. A*, 410 (1969); *J. Phys. Chem.* **75,** 526 (1971).

20. Millman, W. S., and Hall, W. K., *J. Phys. Chem.* **83,** 427 (1979).

21. Peri, J. B., *J. Phys. Chem.* **86,** 1615 (1982).

22. Redey, A., Goldwasser, J., and Hall, W. K., private communications.

23. Caceres, C. V., Fierro, J. L. G., Lopez Agudo, A., Blanco, M. N., and Thomas, H. J., *J. Catal.* **95,** 501 (1985).

24. Valyon, J., and Hall, W. K., *J. Catal.* **84,** 216 (1983).

25. Cotton, F. A., and Wilkinson, G. F. R. S., *in* "Advances Inorganic Chemistry," p. 697. Wiley, New York, 1972.

26. Segawa, K.-I., and Millman, W. S., *J. Catal.* **101,** 218 (1986).

27. Yao, H. C., and Rothschild, W. G., *in* "Proceedings, 4th International Conference on the Chemistry and Uses of Molybdenum," p. 31. Climax Molybdenum Co., Ann Arbor, MI, 1982.